Nearly-room-temperature ferromagnetism and tunable anomalous Hall effect in atomically thin Fe$_4$CoGeTe$_2$

Shaohua Yan,[†,1,2] Hui-Hui He,[†,1,2] Yang Fu,[†,1,2] Ning-Ning Zhao,[1,2] Shangjie Tian,[3,1,2] Qiangwei Yin,[1,2] Fanyu Meng,[1,2] Xinyu Cao,[4] Le Wang,[1,2] Shanshan Chen,[1,2] Ki-Hoon Son,[5] Jun Woo Choi,[5] Hyjin Ryu,[5] Shouguo Wang,[3] Xiao Zhang,[*,4] Kai Liu,[*,1,2] and Hechang Lei[*,1,2]

[1]Department of Physics and Beijing Key Laboratory of Optoelectronic Functional Materials & MicroNano Devices, Renmin University of China, Beijing 100872, China

[2]Key Laboratory of Quantum State Construction and Manipulation (Ministry of Education), Renmin University of China, Beijing 100872, China

[3]School of Materials Science and Engineering, Anhui University, Hefei 230601, China

[4]State Key Laboratory of Information Photonics and Optical Communications & School of Science, Beijing University of Posts and Telecommunications, Beijing 100876, China

[5]Center for Spintronics, Korea Institute of Science and Technology (KIST), Seoul 02792, Korea

Supplemental Information

[†]These authors contributed equally to this work.

[*]Correspondence and requests for materials should be addressed to

X. Z. (zhangxiaobupt@bupt.edu.cn), K. L. (email: kliu@ruc.edu.cn) or H. C. L. (email: hlei@ruc.edu.cn)

Supplementary Figures
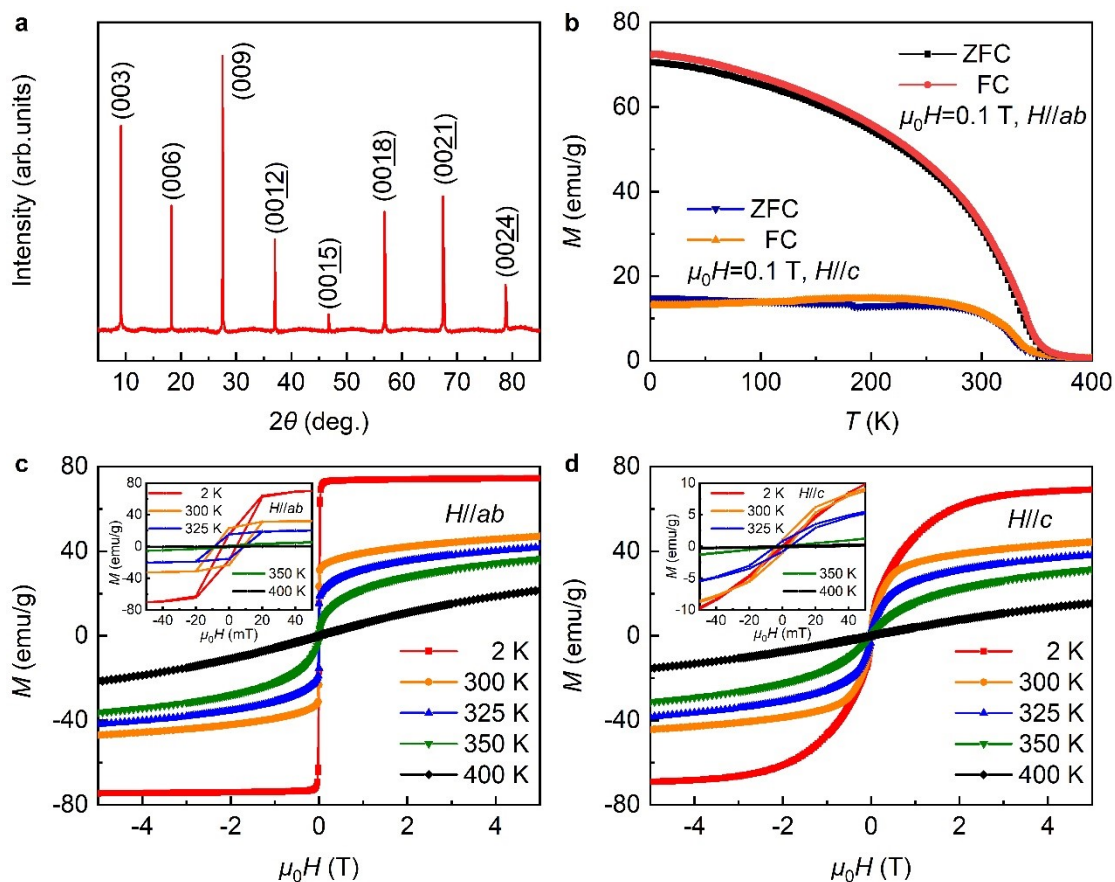
Figure S1. Crystal structure and ferromagnetism of bulk F4CGT. a, XRD pattern of a F4CGT crystal measured using a Bruker D8 X-ray machine with Cu K_α radiation (λ = 0.15418 nm) at room temperature. The crystal surface is parallel to the *ab* plane, consistent with the layered structure of F4CGT. **b**, Temperature dependence of magnetization $M(T)$ for bulk F4CGT crystals at μ_0H = 0.1 T with ZFC and FC modes when *H//ab* and *H//c*. The determined T_Cs from the peak positions of dM/dT curve are about 341 K and 335 K for both field directions. **c** and **d**, Isothermal $M(\mu_0H)$ curves at various temperatures when *H//ab* and *H//c*. Inset in **c** and **d** shows the enlarged part of hysteresis loops at low-field region, respectively. It can be seen that the easy magnetization direction is along the *ab* plane for all of temperatures.
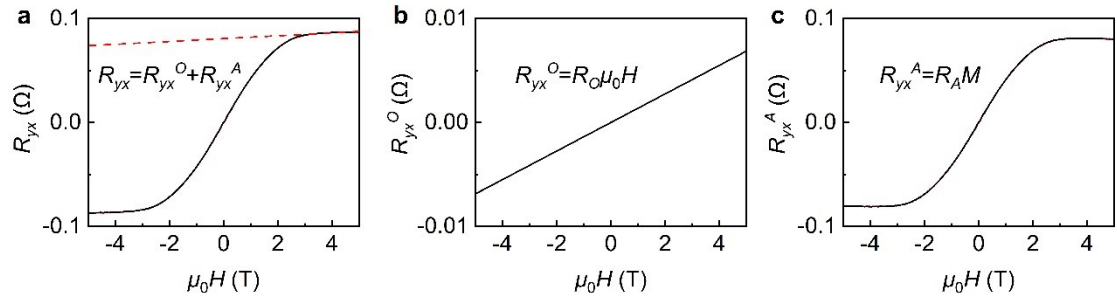
Figure S2. Analysis of ordinary and anomalous Hall resistance. a, The Hall resistance R_{yx} as a function of the magnetic field at 2 K for the sample with $t = 220$ nm. R_0 is derived by linear fitting of data of magnetic field from 3 T to 5 T. **b**, The ordinary Hall resistance R_{yx}^O as a function of the magnetic field. **c**, Field dependence of anomalous Hall resistance R_{yx}^A.
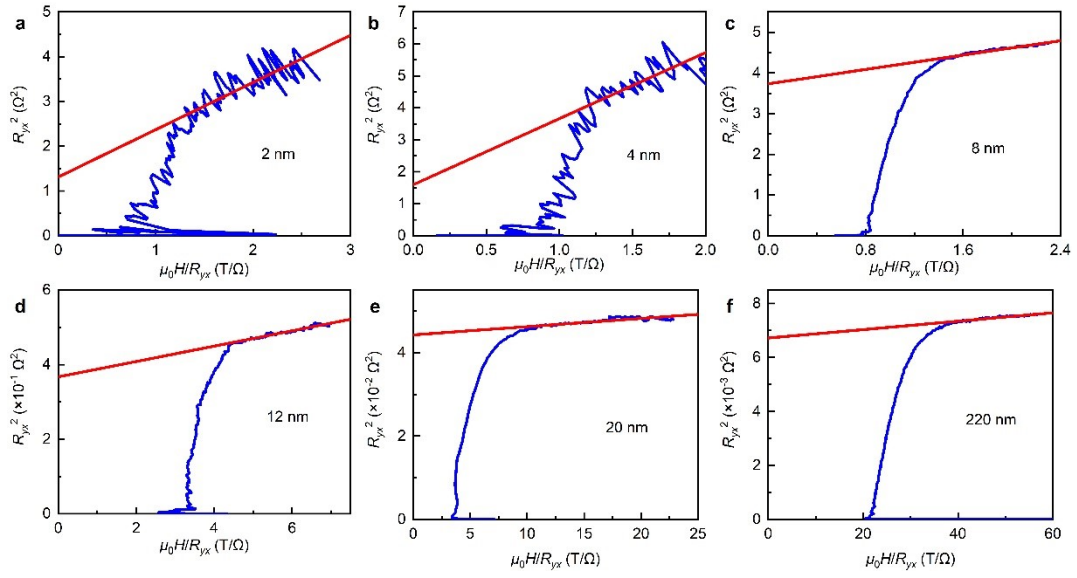
Figure S3. The Arrott plots of F4CGT thin flakes at 2 K. a - f, the F4CGT think flakes with t = 2 nm, 4 nm, 8 nm, 12 nm, 20 nm, and 220 nm. The lines are the linear fits at high-field region.
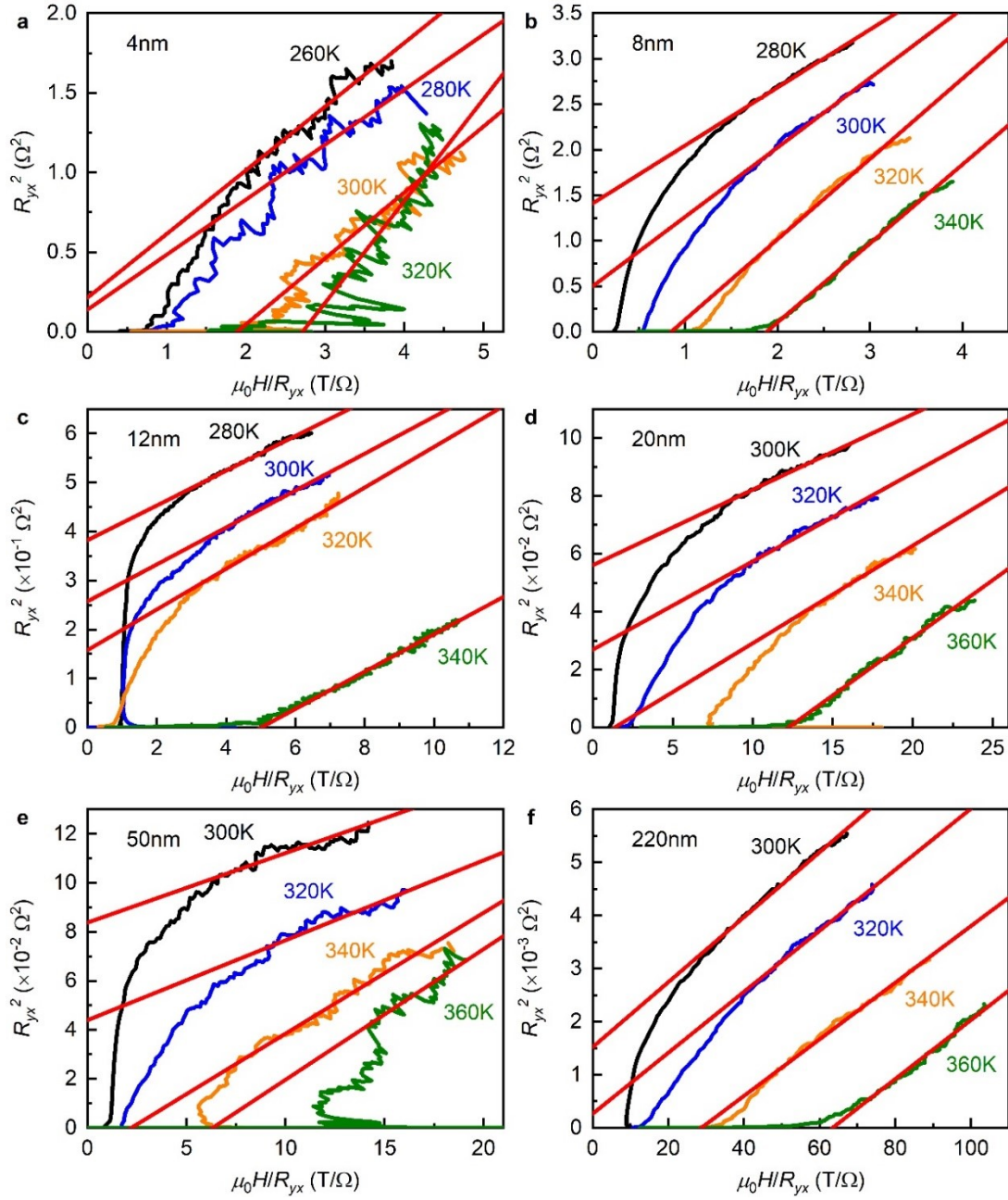
Figure S4. Determining T_c by the analysis of Arrott plots. a - f, Arrott plots of the Hall resistance data for samples with t = 4 nm, 8 nm, 12 nm, 20 nm, 50 nm and 220 nm, respectively. Red lines are linear fits at high magnetic fields. The positive (negative) values of the intercepts to the R_{yx}^2 axis indicate the ferromagnetic (paramagnetic) state.
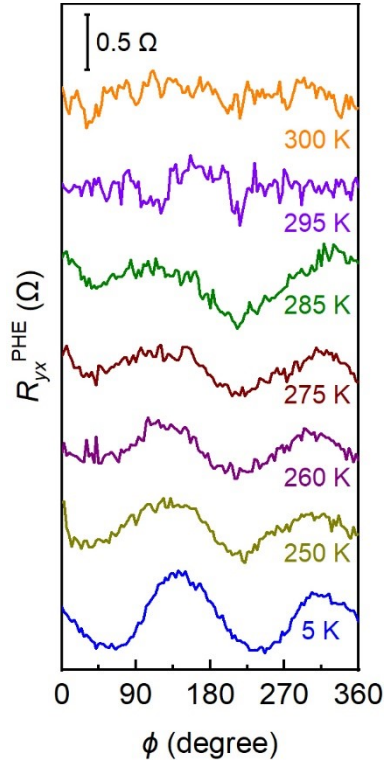
Figure S5. Angular dependence of planar Hall resistance $R_{yx}^{PHE}(\phi)$ with in-plane field $\mu_0 H = 5$ T for the bilayer F4CGT at different temperatures. The data is shifted for clarity.
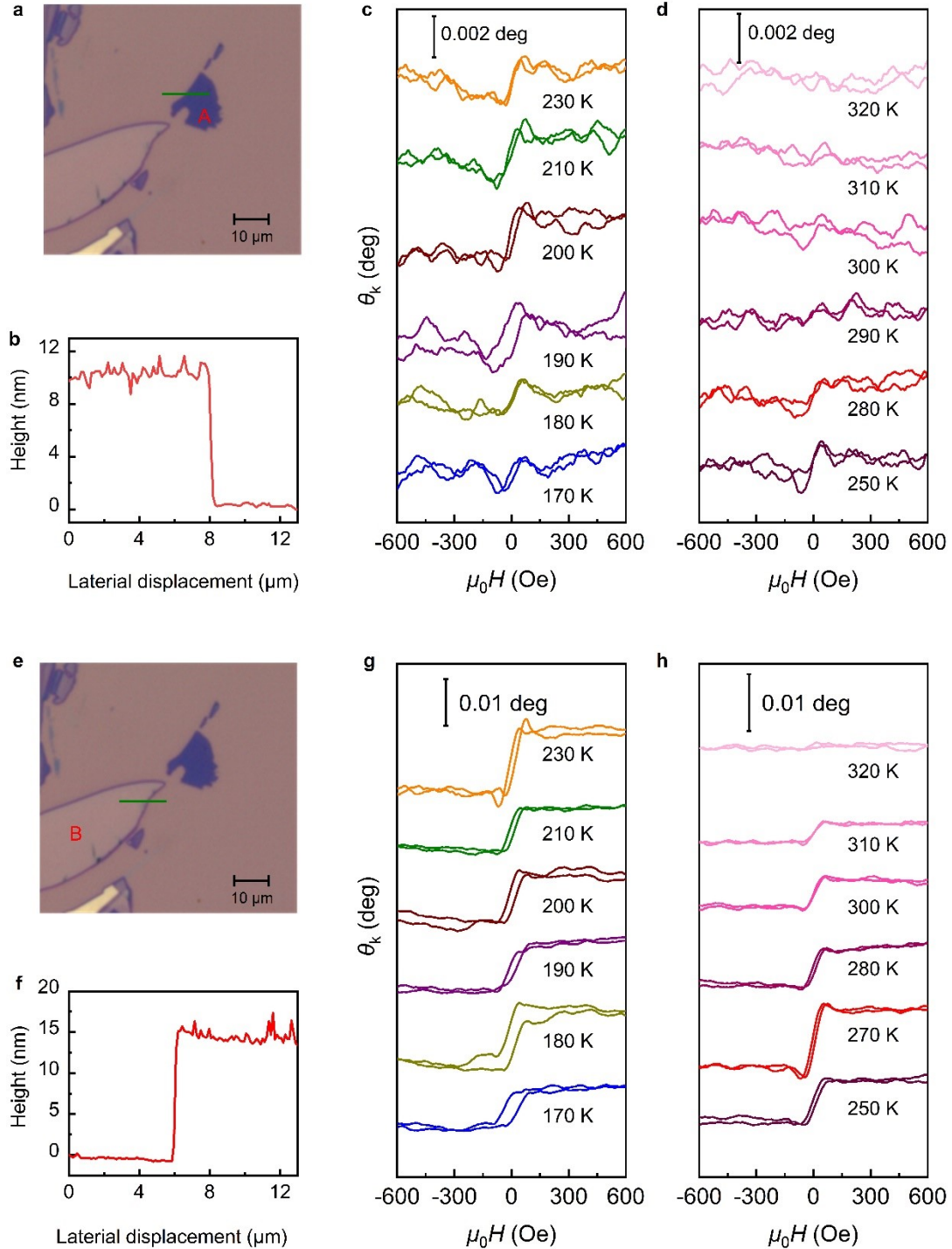
Figure S6. MOKE measurements for F4CGT thin flakes. a, Optical microscope image of a mechanically exfoliated F4CGT flake on a SiO$_2$/Si substrate for $t \sim 10$ nm. **b,** Height profile along the green lines in **a** measured by AFM. **c, d,** Kerr rotation (θ_K) loops as a function of in-plane magnetic field at various temperatures for F4CGT thin flake with $t \sim 10$ nm (A sample in **a**). **e – h,** Corresponding results for F4CGT thin flake with $t \sim 15$ nm (B sample in **e**).
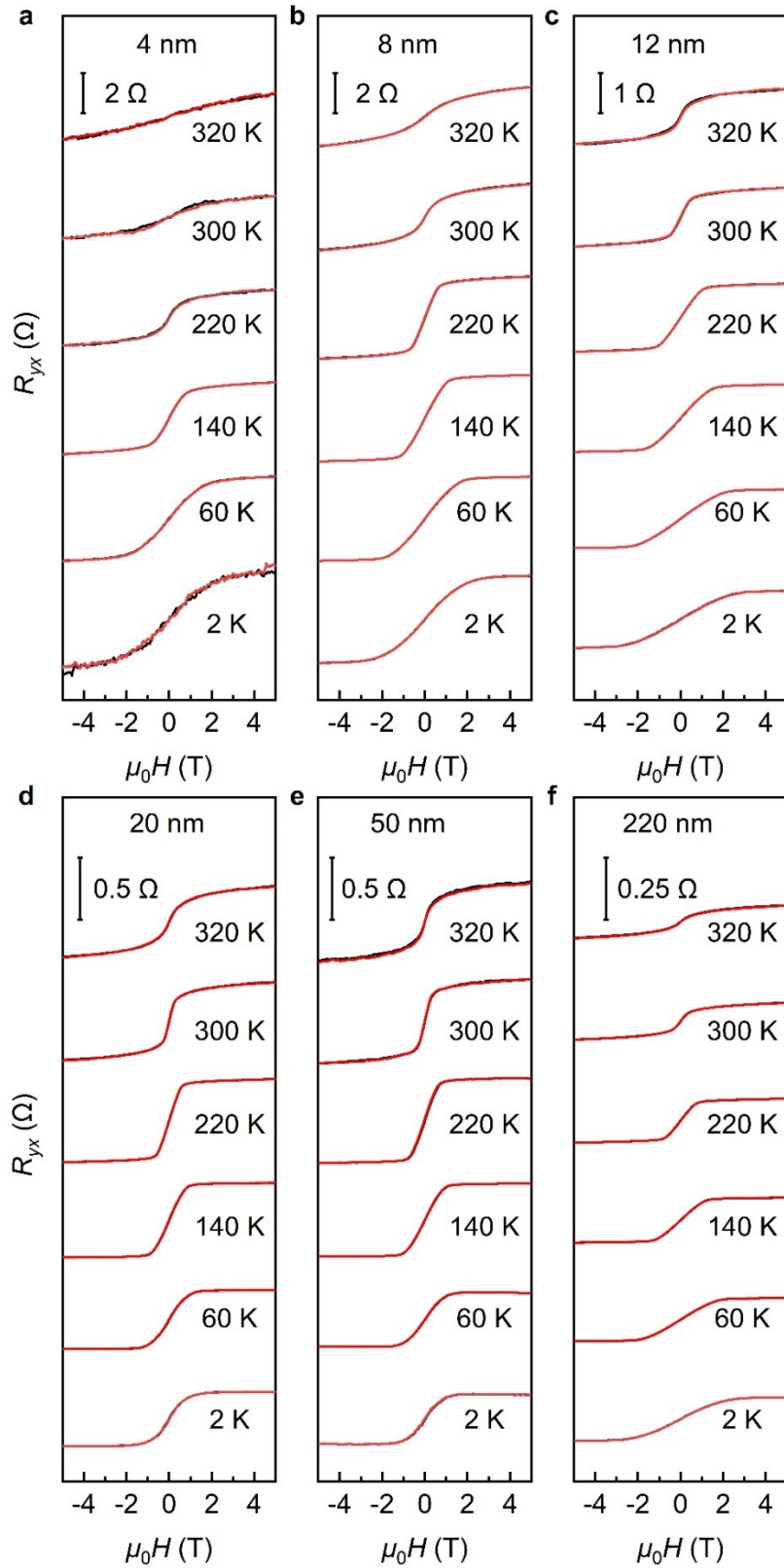
Figure S7. Hall resistance of samples with different *t*. a - f, R_{yx} as a function of magnetic field $\mu_0 H$ at various temperatures for the samples with t = 4 nm, 8 nm, 12 nm, 20 nm, 50 nm and 220 nm. The red and black lines represent the $R_{yx}(\mu_0 H)$ measured when decreasing and increasing fields.
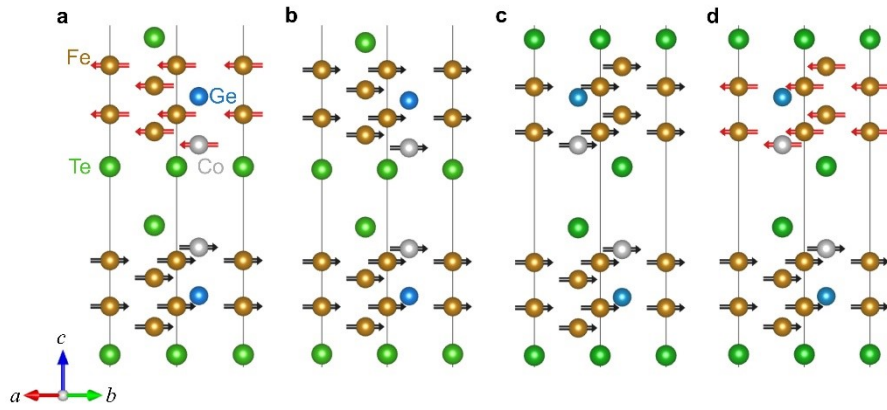
Figure S8. Magnetic configurations in bilayer Fe₄CoGeTe₂ (F4CGT). a, AA-stacking bilayer F4CGT with inter-layer antiferromagnetic coupling and intra-layer ferromagnetic coupling. **b**, AA-stacking bilayer F4CGT with inter-layer and intra-layer ferromagnetic couplings. **c**, AB-stacking bilayer F4CGT with inter-layer and intra-layer ferromagnetic couplings. **d**, AB-stacking bilayer F4CGT with inter-layer antiferromagnetic coupling and intra-layer ferromagnetic coupling. The black and red arrows represent the different spin directions, respectively.
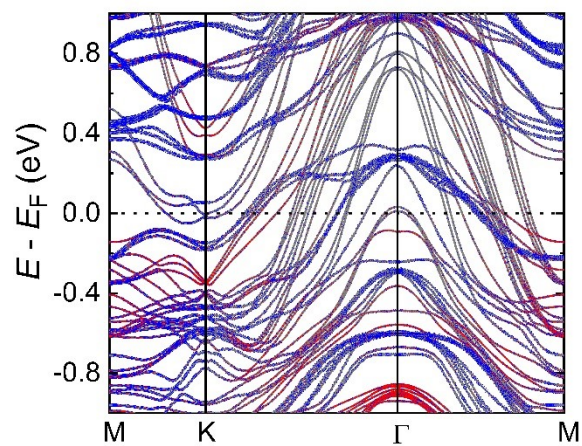
Figure S9. Band structure of bulk F4CGT. The band structure was calculated with the spin-orbit coupling for the ground states (i.e., the in-plane FM state) of ABC-stacking bulk F4CGT with Co occupying at disordered Fe(1) site. The points in red and blue represent to the contributions from Co and Fe atoms, respectively.
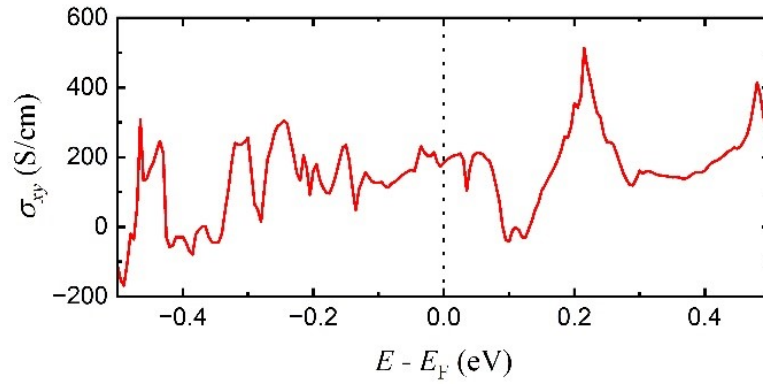
Figure S10. Calculated σ_{xy} of AB-stacking bilayer F4CGT as a function of E - E_F.

Table S1. The calculated relative energies of the NM, FM, and AFM states of bilayer F4CGT (as shown in Figure S8) with respect to the FM states in AA-stacking bilayer F4CGT. The energies are averaged to the ones per formula unit (f.u.).

Energy/f.u.	NM	AFM	FM
AA-stacking	1.379 eV	2.155 meV	0
AB-stacking	1.396 eV	37.135 meV	35.835 meV